



Nanoscale Imaging and Control of Resistance Switching in VO₂ at Room Temperature

Citation

Kim, Jeehoon, Changhyun Ko, Alex Frenzel, Shriram Ramanathan, and Jennifer E. Hoffman.
2010. Nanoscale imaging and control of resistance switching in VO₂ at room temperature.
Applied Physics Letters 96 [213106].

Published Version

doi:10.1063/1.3435466

Permanent link

<http://nrs.harvard.edu/urn-3:HUL.InstRepos:4342532>

Terms of Use

This article was downloaded from Harvard University's DASH repository, and is made available under the terms and conditions applicable to Open Access Policy Articles, as set forth at <http://nrs.harvard.edu/urn-3:HUL.InstRepos:dash.current.terms-of-use#OAP>

Share Your Story

The Harvard community has made this article openly available.
Please share how this access benefits you. [Submit a story](#).

[Accessibility](#)

Nanoscale Imaging and Control of Resistance Switching in VO₂ at Room Temperature

Jeehoon Kim,¹ Changhyun Ko,² Alex Frenzel,¹ Shriram Ramanathan,² and Jennifer E. Hoffman^{1, a)}

¹⁾*Department of Physics, Harvard University, Cambridge, MA 02138, U. S. A.*

²⁾*School of Engineering and Applied Sciences, Harvard University, Cambridge, MA 02138, U. S. A.*

(Dated: 25 May 2010)

We demonstrate controlled local phase switching of a VO₂ film using a biased conducting atomic force microscope tip. After application of an initial, higher ‘training’ voltage, the resistance transition is hysteretic with *IV* loops converging upon repeated voltage sweep. The threshold V_{set} to initiate the insulator-to-metal transition is on order ~ 5 V at room temperature, and increases at low temperature. We image large variations in V_{set} from grain to grain. Our imaging technique opens up the possibility for an understanding of the microscopic mechanism of phase transition in VO₂ as well as its potential relevance to solid state devices.

An insulator-to-metal transition may be triggered in VO₂ as a function of temperature¹, strain², electric field³, or optical excitation⁴. This transition has useful properties such as fast 80 fs switching time⁵, high resistivity ratio, large change in optical reflectance⁶, and tunability near room temperature. Proposed applications include bolometers⁷, memristors⁸, tunable-frequency metamaterials⁹, and data storage¹⁰.

Sensor applications typically require negligible hysteresis, while memory applications call for maximum hysteresis, but all applications seek to maximize the resistivity ratio (RR). Single crystal VO₂ exhibits RR up to 10⁵, but bulk single crystals pose problems for real devices due to cracking on repeated cycle through the transition¹¹. Epitaxial films on insulating Al₂O₃ may have RR up to 10⁴¹². As a route to interface with existing electronics, recent effort has been devoted to film growth on Si substrates¹³, where voltage-controlled switching of VO₂ in capacitor geometry has been demonstrated at room temperature¹⁴. However, the lattice mismatch results in polycrystalline VO₂ films with RR so far limited to $\sim 10^3$. It is therefore important to understand the effects of grain size and the role of grain boundaries in determining hysteresis loop properties RR, V_{set} , and V_{reset} . To date, the voltage triggered transition has been demonstrated down to 200 nm, but only in a fixed area composed of multiple grains¹⁵. Here we present nanoscale images of the voltage-triggered transition: we resolve single grains as small as tens of nanometers.

We study a 200 nm thick VO₂ film grown by rf sputtering from a VO₂ target onto a heavily As-doped Si substrate (*n*-type, with resistivity 0.002 – 0.005 Ω cm)¹⁴. X-ray diffraction data in Fig. 1a corresponds to a polycrystalline, monoclinic VO₂ phase. Fig. 1b shows the thermal phase transition with RR $> 10^2$. From AFM topography, the typical lateral diameter of a VO₂ grain is ~ 100 nm, and the RMS surface roughness is ~ 6 nm.

To investigate this film, we use a home-built force microscope with a conducting cantilever of spring constant

$k_c = 40$ N/m¹⁷. We touch down on the surface with feedback to fix cantilever deflection at a typical setpoint of ~ 4 nm, corresponding to a force of 160 nN, and a pressure of ~ 800 bar (assuming a tip contact area diameter ~ 50 nm). The transition temperature has been shown to shift most significantly with *c*-axis uniaxial stress, at a rate of -1.2 K/kbar¹⁸. The force applied by the tip therefore corresponds to change in local transition temperature ΔT_c of at most 1 K¹⁹.

Upon first upward voltage sweep at a given location, we typically observe a sudden transition from the insulating to the metallic state at a ‘training’ voltage $V_T \sim 12$ V. The transition is hysteretic, returning to the insulating state only at a much lower voltage V_{reset} . Subsequent sweeps show transitions at lower V_{set} , but the hysteresis remains, and *IV* loops roughly stabilize with typical $\sim 5\%$ jitter around $V_{\text{set}} \sim 5$ V and $V_{\text{reset}} \sim 3$ V. This is comparable to the 3% stability of transition temperatures

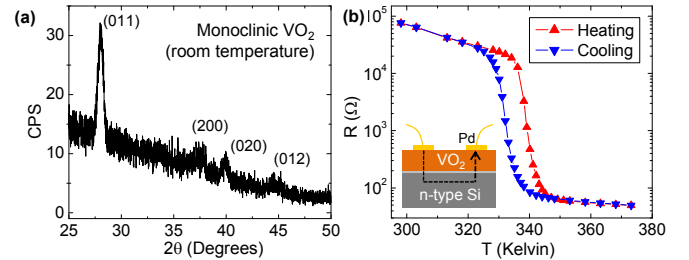


FIG. 1. (Color online) (a) X-ray diffraction (XRD) profile, performed on a Scintag XDS2000 diffractometer using Cu $K\alpha$ radiation ($\lambda \sim 1.5418$ Å) at incidence angle of 1° . The observed peaks correspond to the monoclinic VO₂ phase and demonstrate polycrystallinity.¹⁶ (b) The resistivity ratio is $> 10^2$ as a function of temperature, measured in two-point geometry as shown in the inset. For this data, voltage was applied and current measured between two neighboring $500 \times 500 \mu\text{m}^2$ Pd contact pads, centered 1 mm apart. Varying the distance between Pd pads did not alter the resistance, demonstrating that the resistance is entirely vertical through the VO₂ film, with negligible contribution from the doped Si substrate or the SiO_x interface.

^{a)}Electronic mail: jhoffman@physics.harvard.edu

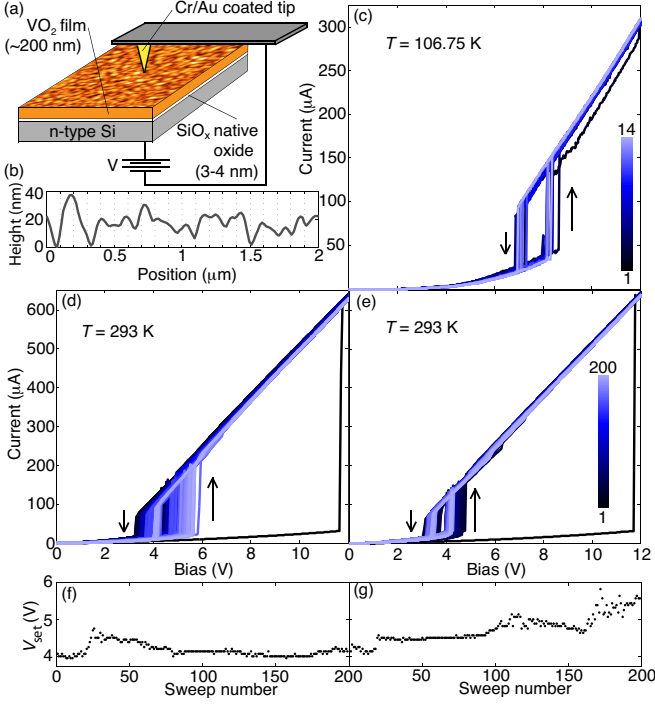


FIG. 2. (Color online) (a) Schematic of the microscope tip and sample geometry. (b) Height trace from AFM topography demonstrates the tip resolution and VO₂ surface roughness. (c) 14 consecutive IV sweeps at a single location at $T = 107$ K. (d-e) 200 consecutive IV sweeps at 2 different representative locations, at room temperature. Iterations start from black and run through light blue. Training voltage is $V_T \sim 12$ V in d-e and > 40 V in c. (f-g) V_{set} as a function of iteration number for the data from d-e.

over 102 thermal cycles previously observed in a macroscopic junction on a VO₂ film on Al₂O₃ substrate²⁰. Typical voltage sweeps are shown in Fig. 2. The following points are worth noting in this unique measurement geometry: (1) Unlike in prior work on 200 nm Au dots¹⁵, we rarely see multiple jumps in a single curve; we really can access single grains! (2) As in this prior work, the measured RR for the entire tip-VO₂-Si structure is limited to < 10 , which we attribute to resistance $R_s \sim 15$ k Ω , in series with the VO₂ film. (3) Loops do not depend on sweep speed from 6 V/s to 16 V/s. (4) Loop characteristics exhibit negligible dependence on force within the range 120 to 420 nN used in this study.

We next investigate the spatial dependence of the transition. After ‘training’ an area by scanning with a bias voltage of 11.1 V, we rescan with increasing bias to watch the details of metallic puddle growth. As shown in Fig. 3, the insulating state displays variations in conductivity up to 100% of the mode value. Conductivity appears constant within each grain, but slowly varies from one grain to the next. Conductivity appears lower in the grain boundaries, which suggests a different stoichiometric phase in the grain boundaries. (We cannot rule out a

topographic artifact from variations in the contact area of the tip between grains and grain boundaries, but such an effect would likely result in increased contact area in the grain boundaries, thus apparent *higher* conductivity.) On increasing voltage, the metallic state nucleates at the grains with largest insulating-state conductivity, grows into a larger metallic puddle, and shrinks again as the voltage is decreased. This type of switching is typically referred to as ‘threshold switching’ (as opposed to ‘memory switching’ in which the resistance state remains changed after removal of the applied voltage). Granularity and lower conductivity grain boundaries remain apparent in the metallic as well as the insulating phase.

Although previous researchers have suggested that field or carrier injection alone may be sufficient to induce the transition^{21,22}, evidence suggests that in our experimental geometry the transition results most directly from Joule heating. At room temperature, the local power injection immediately prior to the insulator-to-metal transition shown in Fig. 2d, is $P \sim 100$ μ W. Given the specific heat $C = 690$ J/(K kg) and the mass density $\rho = 4340$ kg/m³ of VO₂, the time to heat a

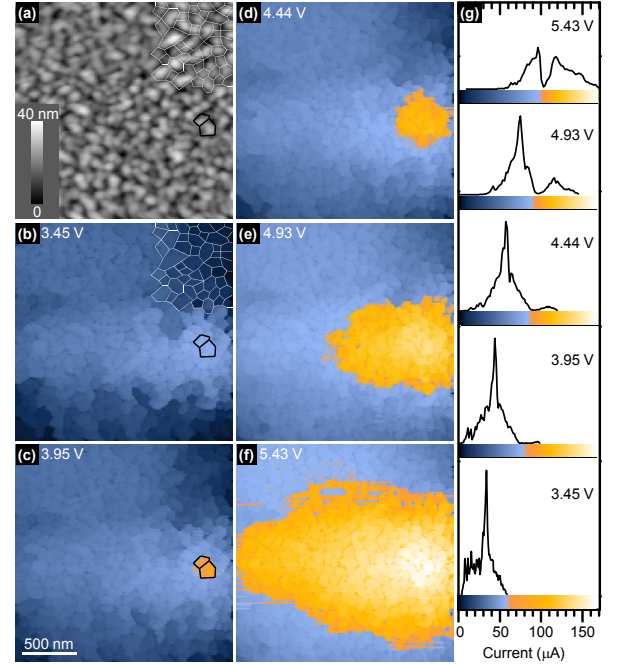


FIG. 3. (Color online) (a) AFM topography of the VO₂ surface. (b-f) Current maps at increasing bias voltage show the metallic puddle seeded at 2 grains (outlined in black), growing with increasing bias. Grain boundaries are drawn in white in the upper right corners of a-b, which were acquired simultaneously, to emphasize the correlation between grain locations and regions of constant current. (g) Current distributions for b-f are bimodal, showing the jump between insulating and metallic state conductivity. A second set of images (not shown), acquired in this same area, as the applied voltage was subsequently decreased by the same increments, show the shrinking and disappearance of the metallic puddle.

single grain of volume $V \sim (100 \text{ nm})^3$ from room temperature ($T_{\text{RT}} \sim 293 \text{ K}$) to the transition temperature ($T_c \sim 340 \text{ K}$) would be only 1.4 ns. The empirical fact that the grain does not transition sooner implies significant thermal conduction away from each grain. The hysteresis may be explained as follows: on upwards voltage sweep, the switching occurs just as the Joule heating exceeds the heat flow out by enough to raise the grain temperature above its T_c . Upon transition, the current flow and resultant Joule heating suddenly increase, so the grain temperature does not immediately drop below T_c as the voltage is swept back down. But the increased Joule heating at the higher current state causes the surrounding grains and Si substrate to also increase in temperature, which increases their thermal conductivity, so heat flows away more quickly. The grain may then return to the insulating state on downwards voltage sweep even though the power input is still higher than the power input on insulator-to-metal transition.

The hypothesis of Joule heating is further suggested by the following observations: (1) Transition occurs at the same absolute value of voltage, to within $\pm 10\%$, for positive and negative applied bias. (2) The transition is seeded at the grains with the largest insulating state conductance (i.e. the largest Joule heating for a given applied voltage). (3) The transition can also be triggered by voltage at the much reduced global temperature of 107 K, as shown in Fig. 2c, but the transition is shifted to higher voltage and power, as would be required to achieve the much larger $\Delta T = 234 \text{ K}$.

The origin of the training voltage remains unknown. We rule out surface contamination, because use of the tip to scrape the VO_2 surface, in situ in vacuum, with enough force to physically remove up to 10% of the VO_2 material, does not lower the initial transition voltage. Possibly, the training alters the native SiO_x layer. More likely, the training may occur within the VO_2 film itself, possibly due to O migration which improves grain stoichiometry, or due to formation of more conductive phases such as Magneli ($\text{V}_n\text{O}_{2n-1}$) phases²³ in the grain boundaries.

In conclusion, single grain switching with reproducible hysteresis demonstrates the scaling of the insulator-to-metal transition in VO_2 down to tens of nanometers. Nanoscale voltage-triggered switching at room temperature may lead to additional VO_2 applications. High resolution conductance imaging of VO_2 has the potential to elucidate the microscopic mechanism of phase transition, and to inform the optimization of grain size and grain

boundary composition in practical VO_2 film devices.

This work is supported by the Harvard NSEC under NSF Grant No. PHY-0117795, and by AFOSR Grant No. FA9550-08-1-0203.

- ¹F. J. Morin, Physical Review Letters **3**, 34 (1959).
- ²J. Cao, E. Ertekin, V. Srinivasan, W. Fan, S. Huang, H. Zheng, J. W. L. Yim, D. R. Khanal, D. F. Ogletree, J. C. Grossman, and J. Wu, Nature Nanotechnology **4**, 732 (2009).
- ³G. Stefanovich, A. Pergament, and D. Stefanovich, J. Phys.: Condens. Matter **12**, 8837 (2000).
- ⁴A. Cavalleri, C. Tóth, C. Siders, J. A. Squier, F. Ráksi, P. Forget, and J. C. Kieffer, Physical Review Letters **87**, 237401 (2001).
- ⁵A. Cavalleri, T. Dekorsy, H. H. W. Chong, J. C. Kieffer, and R. W. Schoenlein, Physical Review B **70**, 161102 (2004).
- ⁶D. Ruzmetov, K. T. Zawilski, S. D. Senanayake, V. Narayanamurti, and S. Ramanathan, Journal of Physics: Condensed Matter **20**, 465204 (2008).
- ⁷C. Chen and Z. Zhou, Applied Physics Letters **91**, 011107 (2007).
- ⁸T. Driscoll, H.-T. Kim, B.-G. Chae, M. D. Ventra, and D. N. Basov, Applied Physics Letters **95**, 043503 (2009).
- ⁹T. Driscoll, S. Palit, M. M. Qazilbash, M. Brehm, F. Keilmann, B.-G. Chae, S.-J. Yun, H.-T. Kim, S. Y. Cho, N. M. Jokerst, D. R. Smith, and D. N. Basov, Applied Physics Letters **93**, 024101 (2008).
- ¹⁰M.-J. Lee, Y. Park, D.-S. Suh, E.-H. Lee, S. Seo, D.-C. Kim, R. Jung, B.-S. Kang, S.-E. Ahn, C. B. Lee, D. H. Seo, Y.-K. Cha, I.-K. Yoo, J.-S. Kim, and B. H. Park, Advanced Materials **19**, 3919 (2007).
- ¹¹J. A. S. Barker, H. W. Verleur, and H. J. Guggenheim, Phys. Rev. Lett. **17**, 1286 (1966).
- ¹²M. M. Qazilbash, M. Brehm, B.-G. Chae, P.-C. Ho, G. O. Andreev, B.-J. Kim, S. J. Yun, A. V. Balatsky, M. B. Maple, F. Keilmann, H.-T. Kim, and D. N. Basov, Science **318**, 1750 (2007).
- ¹³D. Ruzmetov, K. T. Zawilski, V. Narayanamurti, and S. Ramanathan, Journal of Applied Physics **102**, 113715 (2007).
- ¹⁴C. Ko and S. Ramanathan, Journal of Applied Physics **106**, 034101 (2009).
- ¹⁵D. Ruzmetov, G. Gopalakrishnan, J. Deng, V. Narayanamurti, and S. Ramanathan, Journal of Applied Physics **106**, 083702 (2009).
- ¹⁶JCPDS Card No. 01-082-0661.
- ¹⁷<http://www.spmtools.com/nsc/16/cr-au>.
- ¹⁸L. A. Ladd and W. Paul, Solid State Communications **7**, 425 (1969).
- ¹⁹Our attempts to use smaller forces with $k_c = 0.15 \text{ N/m}$ and $k_c = 3 \text{ N/m}$ spring constant cantilevers did not result in reproducible resistance measurements.
- ²⁰C. Ko and S. Ramanathan, Journal of Applied Physics **104**, 086105 (2008).
- ²¹G. Gopalakrishnan, D. Ruzmetov, and S. Ramanathan, J. Mater. Sci. **44**, 5345 (2009).
- ²²M. M. Qazilbash, Z. Q. Li, V. Podzorov, M. Brehm, F. Keilmann, B. G. Chae, H. T. Kim, and D. N. Basov, Applied Physics Letters **92**, 241906 (2008).
- ²³S. Kachi, K. Kosuge, and H. Okinaka, J. Solid State Chem. **6**, 258 (1973).